Appendix A

A New Upper Limit To The Abundance Ratio Of Atomic Deuterium to Hydrogen In The Direction Of The Galactic Centre

Astron. Astrophys. 79, L9-L11 (1979)

ASTRONOMY AND ASTROPHYSICS

Letter to the Editor

A New Upper Limit to the Abundance Ratio of Atomic Deuterium to Hydrogen in the Direction of the Galactic Centre

K. R. Anantharamaiah and V. Radhakrishnan

Raman Research Institute, Bangalore-560006, India

Received April 17, 1979

SUMMARY. We report a new upper limit for the strength of the 327 MHz absorption line of deuterium in the direction of the galactic centre. Our observations do not confirm the possible detection of this line reported by Cesarsky et al (1973) and Pasachoff and Cesarsky (1974). We obtain an upper limit of 5.8×10^{-5} for the atomic D/H ratio by correlating the observed spectrum with the HI absorption spectrum of Sgr A. This limit is comparable to that of Weinreb (1962) of 8×10^{-5} for the direction of Cas A, and compatible with the direct measurement of the D/H ratio in nearby interstellar clouds from UV observations by the Copernicus satellite.

Key Words: Deuterium, Galactic Centre, Sgr A, Interstellar gas.

INTRODUCTION

The astrophysical importance of the deuterium to hydrogen abundance ratio, D/H, and the extremely high hydrogen optical depth towards the galactic centre have prompted several attempts in the past to detect the ground state hyperfine transition of deuterium at 327 MHz in this direction (see Cesarsky et al 1973). A possible detection of this line in absorption towards the galactic centre and a further compatible observation have been reported by Cesarsky et al (1973) and Pasachoff and Cesarsky (1974). However, recent observations of Sarma and Mohanty (1978) do not show any positive detection.

We report in this note a further attempt to detect this line in the same direction using the Ooty Radio Telescope described by Swarup et al (1971).

OBSERVATIONS AND ANALYSIS

The 530 m x 30 m Ooty Radio Telescope operates at a nominal centre frequency of 326.5 MHz and has an HPBW of $5.6 \cos \delta$ arcmin in the north-south and 2° in the east-west direction in the total power mode of operation. With the new RF amplifiers, installed recently, the system temperature is now about 250 °K when the antenna is pointed towards a cold region in the sky. The observations were carried out using a 36-channel filter bank receiver as the back-end, having a 2.5 KHz (2.3 km s^{-1}) filter bandwidth and 3 KHz (2.7 km s^{-1}) filter separation. A frequency synthesizer operated from a rubidium frequency standard was used as the first local oscillator.

Observations were made during two major observing sessions in June 1978 and July 1978 totalling about 84 hours of data. Interference was noticed in only a few records and these were rejected. During the initial observations, simple frequency switching was employed in which the first local oscillator was switched every 200 ms between an on-line frequency (ON) and a reference frequency 120 KHz away. This resulted in a baseline slope which is natural to any phased array because of the slight beam shift produced when the frequency of the first local oscillator is altered. To minimise this slope during the subsequent observations, data was acquired in a double frequency switched mode; the first local oscillator was switched between an on-line frequency and two reference frequencies (REF1, REF2) on either side of the on-line frequency in the sequence ON-REF1-ON-REF2-ON- etc., spending 200 ms on each frequency. LSR corrections were applied as necessary to keep the 0 km s^{-1} velocity channel for the deuterium line located at the centre of the filter bank.

Data was acquired only while tracking the region Sgr A ($\alpha = 17^h42^m30^s$, $\delta = -28\ 59'$ (1950)) over an hour angle range generally between -3^h30^m and 5^h0^m. Each individual day's data was analysed to obtain the spectrum for that day. These one-day spectra were averaged with weighting factors proportional to their integration time. A linear baseline with a slope of 0.19×10^{-4} (km s^{-1})$^{-1}$ was fitted to the outer 12 channels of the averaged spectrum to get the final integrated spectrum shown in Fig. 1. The total integration time for this spectrum is 2.737×10^5s.

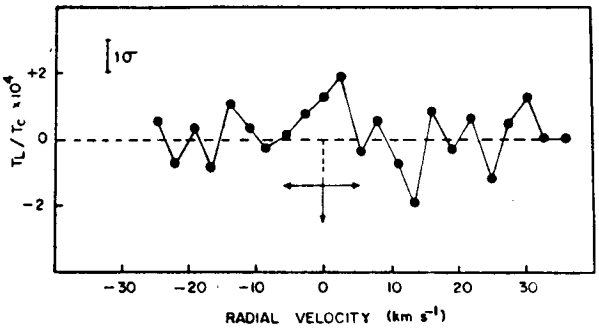

Fig. 1. Spectrum in the direction of Sgr A at the frequency of the deuterium line. The filter bandwidth was 2.3 km s^{-1} and the ordinate is in units of optical depth. The position and full width at half optical depth of the HI absorption component used for the correlation (see text) is also indicated.

INTERPRETATION OF THE OBSERVATIONS AND DISCUSSION

We have plotted in the ordinate of Fig. 1 the antenna temperature in the line (T_L) divided by the antenna temperature due to the continuum background

Send offprint requests to: V. Radhakrishnan

source (T_C). The points in the plot of Fig. 1 show an rms fluctuation of 0.93×10^{-4} as against the theoretically estimated value of 1.04×10^{-4} expected in the absence of any spectral line. No feature above 2.5σ is seen in the spectrum. This implies an upper limit of 2.3×10^{-4} (2.5σ) for T_L/T_C for the deuterium line, in the direction of the galactic centre.

In view of the number of references in the literature for the abundance ratio D/H in the direction of the galactic centre, we compare our observations with those of Cesarsky et al (1973) and Sarma and Mohanty (1978). In their analysis Cesarsky et al (1973) use the relation $\tau_D = -T_L/fT_C$ where 'a fraction f of the observed continuum radiation originates behind an absorbing cloud of optical depth τ_D in the deuterium line and τ_H in the hydrogen line'. We show in Fig. 2a and Fig. 2b the spectra reported by Pasachoff and Cesarsky (1974) and Sarma and Mohanty (1978). In Fig. 2c we show our spectrum smoothed to the same resolution (4.5 km s^{-1}) and with T_L/fT_C plotted in the ordinate for comparison purposes. The value of f for Fig. 2a is 0.4 and for Fig. 2b and Fig. 2c is 0.77 (instead of 0.56 used by Sarma and Mohanty (1978); they used fT_S instead of fT_C in their plots). As can be seen from the figure, we do not find any evidence in our spectrum for the dip at -4 km s^{-1} seen in the spectrum of Pasachoff and Cesarsky (1974).

To estimate an upper limit to the abundance ratio D/H, of deuterium to hydrogen, we assume, in the

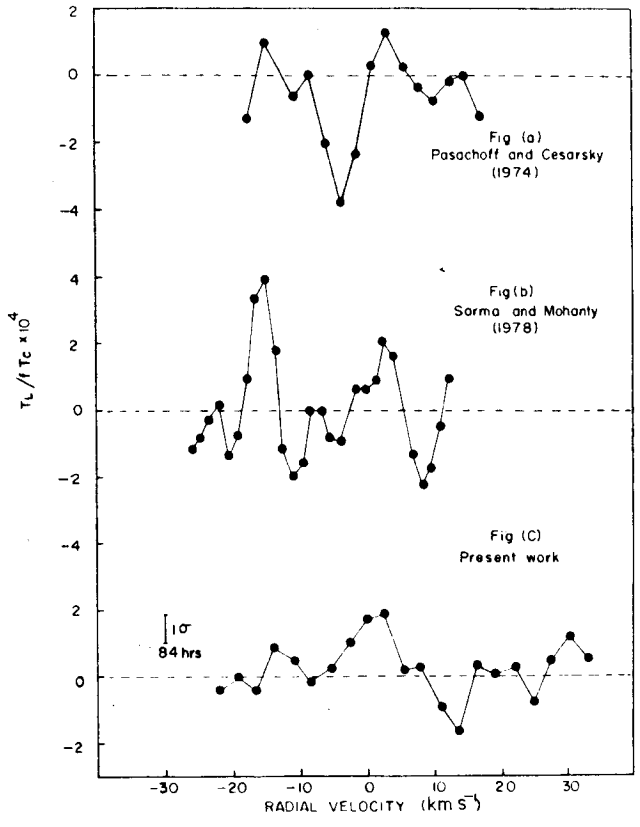

Fig. 2. A comparison of various observations in the direction of Sgr A at the deuterium line frequency. The observations reported in this paper are shown in Fig. 2c smoothed to the same resolution (4.5 km s^{-1}) as reported for the observations in 2a and 2b. The ordinates were also chosen to make the observations directly comparable as explained in the text.

absence of any positive detection of the deuterium line, that whatever deuterium is present in the interstellar gas between us and the galactic centre is distributed in the same way as neutral atomic hydrogen. A knowledge of the optical depth in the 21 cm hydrogen line, in this direction to the required accuracy was hitherto lacking. However, a recent analysis by Radhakrishnan and Sarma (1979) of an interferometer measurement obtained with the Parkes Interferometer (Radhakrishnan et al, 1972) has provided a very reliable estimate of the parameters of the 21 cm absorption components in the spectrum of Sgr A. The high S/N ratio in the wings of the deep central feature was used to determine its peak optical depth of 4.3, its mean velocity of -0.2 km s^{-1} and a full width at half maximum optical depth of 11.8 km s^{-1}.

In our analysis we further assume that the optical depth due to hydrogen over such a long path length in the plane is, to first order, independent of the direction. This assumption is based on the statistical study of Radhakrishnan and Goss (1972) in which they conclude that neutral hydrogen appears in cloud concentrations, of which there are at least 2.5 per kpc in any line of sight along the plane. The above assumption, therefore, is likely to cause errors only as a result of differential galactic rotation altering the shape of the hydrogen absorption profile, whose area however, should depend on the distance only. We have estimated the magnitude of possible lowering of the peak optical depth over the angle of the continuum source, taking account of the decrease in intensity of the continuum radiation away from the central peak. We find this effect to be negligible and correspondingly analyse our results on the assumption that the parameters of the 21 cm absorption profile that would be obtained with the antenna beam of the Ooty telescope would be essentially the same as found from the Parkes measurement referred to above. To estimate the optical depth in the deuterium line we have used the simple relation $\tau_D = -T_L/T_C$, and to estimate an upper limit for D/H a value of 4.3 for the 21 cm hydrogen optical depth. The appropriateness of this value of 21 cm optical depth for the present purpose has been discussed by Radhakrishnan and Sarma (1979).

From the above assumptions it follows that in our spectrum of Fig. 1, the deuterium profile, if present, should resemble the hydrogen profile discussed above. The velocity width of the deuterium profile should be same as that of the hydrogen profile since the broadening of the latter must clearly be due to the external motions of the large number of clouds along the line of sight; the line widths of individual clouds are much smaller as determined from studies in other directions of the galaxy.

We have accordingly correlated the deuterium spectrum shown in Fig. 1 with the 11.8 km s^{-1} wide component centred at -0.2 km s^{-1} in the HI absorption spectrum. This component was least-square fitted to the deuterium spectrum by varying its peak optical depth.

The best fit was obtained for a peak optical depth of $(-2.3 \pm 3.0) \times 10^{-4}$. The errors quoted are the 95% confidence limits from a Chi-square goodness-of-fit test and indicate an upper limit for the deuterium optical depth of 0.7×10^{-4}; using the value for $\tau_H = 4.3$ referred to earlier, we get an upper limit for the ratio of the optical depths τ_D/τ_H of 1.6×10^{-5}.

The relationship between the ratio of optical depths in the deuterium and hydrogen lines and the

ratio of their column densities has been discussed by Weinreb (1962), who showed that $\tau_D/\tau_H = 0.33 \times N_D/N_H$ on the assumption that half of the doppler broadened width of the lines arises due to thermal motions. We have shown above that thermal broadening must contribute negligibly to the line widths in this case, and the appropriate relation becomes $\tau_D/\tau_H = 0.28 \times N_D/N_H$. Using this we get the 95% confidence upper limit for the mean abundance ratio of atomic deuterium to hydrogen in the interstellar gas between us and the galactic centre as 5.8×10^{-5}.

COMPARISON WITH OTHER OBSERVATIONS AND CONCLUSIONS

Our upper limit is comparable to the upper limit of 8×10^{-5} obtained by Weinreb (1962) in a notable attempt to measure this line in the direction of Cas A. Direct and unambiguous determination of the atomic deuterium to hydrogen ratio in nearby interstellar space has been made with the Copernicus satellite by observing the Lyman absorption lines of atomic D and H in the direction of several stars ranging in distance between 1 and 1,000 parsecs (York and Rogerson 1976, Vidal-Madjar et al 1977, Dupree et al 1977). In the 9 directions for which these lines are observed, the abundance ratio D/H has an unexpected scatter with values ranging from 2×10^{-6} to 4×10^{-5} and a mean value around 2×10^{-5}. These results seem to indicate that even if the highest D/H ratio observed by Copernicus were typical of all the clouds along the 10 kpc pathlength between us and the galactic centre, we would still have failed to detect the line.

If we assume that the clouds observed by Copernicus are typical of those found in the direction to the galactic centre, we should expect a D/H ratio of the mean value referred to above, namely 2×10^{-5}. The unambiguous detection in the 327 MHz absorption line of a value one third of our upper limit would require an increase in observing time of at least an order of magnitude over the 84 hours taken for the present observation. As the continuum radiation from the source Sgr A dominates system noise for most large radio telescopes no improvement can be expected with even larger collecting areas. It also appears that unless the atomic D/H ratio were anomalously higher in certain clouds, by over an order of magnitude, it would be even more difficult to detect this line in absorption against continuum sources in other directions where differential galactic rotation would contribute to reducing the value of the peak optical depth.

ACKNOWLEDGEMENTS

We wish to thank R.S. Arora and D.K. Ravindra for the construction and testing of the first local oscillator system used in our observations. Prof. G. Swarup kindly provided the facilities at the Radio Astronomy Centre, Ooty operated by the Tata Institute of Fundamental Research, Bombay. We thank N.A. Rajagopalan for his help in the data analysis and Rajaram Nityananda and N.V.G. Sarma for useful discussions.

REFERENCES

Cesarsky, D.A., Moffet, A.T., Pasachoff, J.M.: 1973, Astrophys. J. Lett. 180, L1

Dupree, A.K., Baliunas, S.L., Shipman, H.L.: 1977, Astrophys. J. 218, 361.

Pasachoff, J.M., Cesarsky, D.A.: 1974, Astrophys. J. 193, 65.

Radhakrishnan, V., Goss, W.M., Murray, J.D., Brooks, J.W.: 1972, Astrophys. J. Suppl. 24, 49.

Radhakrishnan, V., Sarma, N.V.G.: (to be published)

Sarma, N.V.G., Mohanty, D.K.: 1978, Mon. Not. Roy. Astron. Soc., 184, 181.

Swarup, G., Sarma, N.V.G., Joshi, M.N., Kapahi, V.K., Bagri, D.S., Damle, S.H., Ananthakrishnan, S., Balasubramaniam, V., Bhave, S.S., Sinha, R.P.: 1971, Nature Phys. Sci. 230, 185.

Vidal-Madjar, A., Laurent, C., Bonnet, R.M., York, D.G.: 1977, Astrophys. J. 211, 91.

York, D.G., Rogerson, J.B.: 1976, Astrophys. J. 203, 378.

Weinreb, S.: 1972, Nature, 195, 367.

Appendix B

On The Statistics Of Galactic HI Clouds

From The Proceedings of The Second Regional Meeting of The IAU, Bandung, Indonesia, August 1981.

ON THE STATISTICS OF GALACTIC HI CLOUDS

K.R. Anantharamaiah, V. Radhakrishnan
Raman Research Institute, Bangalore-560080, India
and
P.A. Shaver
European Southern Observatory Karl-Schwarzschild-Strasse 2
D-8046 Garching bei Munchen, FRG

ABSTRACT

The number density and random motions of interstellar HI clouds have been studied using an entirely novel method involving the comparison of the terminal velocities of HI absorption spectra in the direction of HII regions with their recombination line velocities. We confirm the conclusions of an earlier study attributing these velocity differences mainly to the random motions of the clouds. We also show that these motions are better described in terms of two populations with quite different velocity dispersions than by a single population with an exponential distribution of velocities. The present analysis yields estimates of the number densities and dispersions of $n_s = 7.7 \pm 1.8$ kpc^{-1} $\sigma_s = 4.1 \pm 0.7$ kms^{-1} for the "slow" clouds, and $n_f = 0.6 \pm 0.15$ kpc^{-1}, $\sigma_f = 15.2 \pm 3.2$ kms^{-1} for the "fast" clouds. These values are compared with earlier estimates and the implications discussed. It is concluded that the values for the slow clouds are an improvement over earlier determinations, but that those for the population of fast clouds are underestimates because of selection effects in the data used.

1. INTRODUCTION

The radial velocities of interstellar clouds do not conform strictly to the predictions of the Schmidt model of galactic rotation. This is because there are non-systematic or random motions in addition to the systematic circular motions around the centre of the galaxy. The magnitude of these random motions can in principle be estimated by comparing the measured radial velocities with the predicted radial velocities if the distances to the clouds could somehow be determined independently. While this is almost impossible in practice for distant clouds in the galactic plane, a similar comparison can be made with HI absorption measurements against background continuum sources with independent radial velocity determinations. In such cases, one could compare the radial velocity of the background continuum source with the terminal velocity (corresponding to the greatest distance) of the HI absorption spectrum of the source. If there were no random motions, one would expect only the velocity difference corresponding to the distance between the background source and the HI cloud nearest to, and in front of it: the magnitude of this difference would depend on the galactic longitude.

Shaver et al (1981, hereinafter referred to as paper I) have made such a comparison. The recombination line velocity of each of 38 HII regions of known distance

Table 1. Parameters for the 38 HII Regions (1)

Source		$\Delta V^{(2)}$ km s^{-1}	$\tau_{max}{}^{(3)}$	Distance(4) kpc	$(dv/dr)^{(5)}$ kms^{-1} kpc^{-1}
G	Optical				
206.5-16.4	NGC 2024	+3.7	5.3	0.5	10.8
209.0-19.4	Orion	+8.3	1.05	0.5	11.4
243.1+0.4	RCW 16	+1.4	>0.7	4.2	12.5
265.1+1.5	RCW 36	+2.0	3.5	0.6	6.1
268.0-1.1	RCW 38	+5.3	4.3	0.6	6.6
274.0-1.1	RCW 42	- 3	~1.2	6.1	11.8
282.0-1.2		- 2.4	~1.0	6.6	11.3
284.3-0.3	RCW 49	+4.7	~3.0	6.0	9.5
298.2-0.3		- 2.4	~2.5	11.7	13.4
298.9-0.4		+0.8	~1.5	11.5	13.6
322.2+0.6	RCW 92	+4.2	~2.3	3.7	-13.5
326.6+0.6	Nebulosity	+2.5	~1.0	3.2	-14.6
327.3-0.6	RCW 97	+0.7	2.9	3.5	-14.6
330.9-0.4		+6.9	>0.9	4.2	-15.0
332.2-0.4		+1	~1.6	4.1	-15.0
333.1-0.4		- 0.9	2.2	4.1	-15.0
333.6-0.2	Nebulosity	+21.7	~1.2	3.7	-15.5
336.5-1.5	RCW 108	+1.1	~2.3	2.1	-12.5
337.9-0.5		+19.6	~0.3	3.5	-14.6
338.9+0.6		- 1	>1.2	5.2	-15.9
340.8-1.0	RCW 110	+3.2	~1.6	2.5	-11.5
345.4-0.9	RCW 117	+10.5	1.5	5.0	-11.0
345.4+1.4	Nebulosity	+9.4	~1.2	1.9	-8.6
348.7-1.0	RCW 122	+27.2	0.2	2.0	-12.5
351.4+0.7	NGC 6334	+1.8	1.5	0.7	-4.7
351.7-1.2		+16.5	3.5	2.6	-9.6
353.1+0.7	NGC 6357	+0.9	~1.6	1.0	-3.8
353.2+0.9	NGC 6357	+7.2	~1.0	1.0	-3.8
6.0 - 1.2	M8	+12.4	0.44	1.0	3.5
12.8-02		0.0	2.9	4.6	11.2
15.0-07	M17	+4.6	~1.4	2.3	9.2
16.9+0.7	M16	- 5.0	1.3	2.7	9.9
25.4-0.2		+6.0	0.2	4.7	15.6
28.8+3.5	RCW 174	+6.5	2.5	0.1	12.6
30.8-0.0		+4.9	1.3	7.0	6.2
34.3+0.1		+2.1	>1.2	3.8	14.3
35.2-1.8		- 2.2	3.5	3.4	14.5
111.5+0.8	S158	+1.4	-	4.9	-12.3

Notes to Table 1:

1. See Shaver et al (1981) for references.
2. ΔV is positive when the HI velocity corresponds to a greater distance than that of the H 109α line.
3. τ_{max} is the optical depth of the extreme HI absorption feature.
4. Distances are based on recombination line velocity.
5. Computed near the HII region.

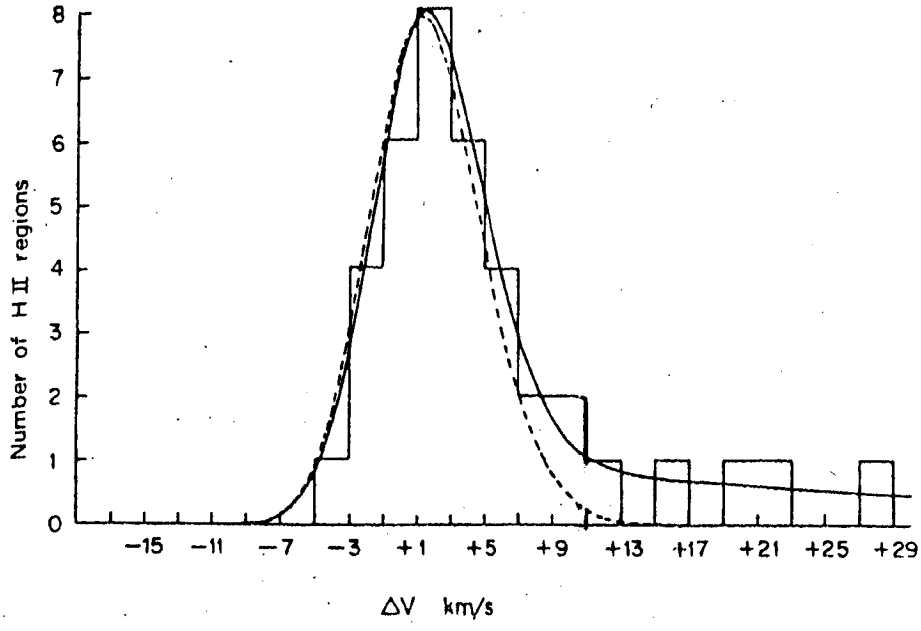

Figure 1. (Taken from Shaver et al 1981). Histogram of the difference between the H 109α velocity and that of the extreme HI absorption feature (corresponding to the greatest distance) for 38 galactic HII regions. The dashed line is the fit obtained by Shaver et al (1981) considering the dispersion of normal clouds only; the solid line includes the effect of a small fraction of clouds with much larger random motions.

was compared with the terminal velocity of its HI absorption spectrum (Table 1). Figure 1 shows a histogram of the velocity differences from paper I. Shaver et al (paper I) found that in most (80%) of the cases, the velocity of the HI absorption feature corresponds paradoxically to a *greater* distance than that of the HII region. They showed that this was simply a consequence of the random motions of the clouds, and that in these cases the values of ΔV (the difference between the recombination line velocity and extreme HI velocity) must provide *lower limits* to such motions. On account of these motion, some clouds will appear to be beyond the HII region as illustrated in Fig. 2.

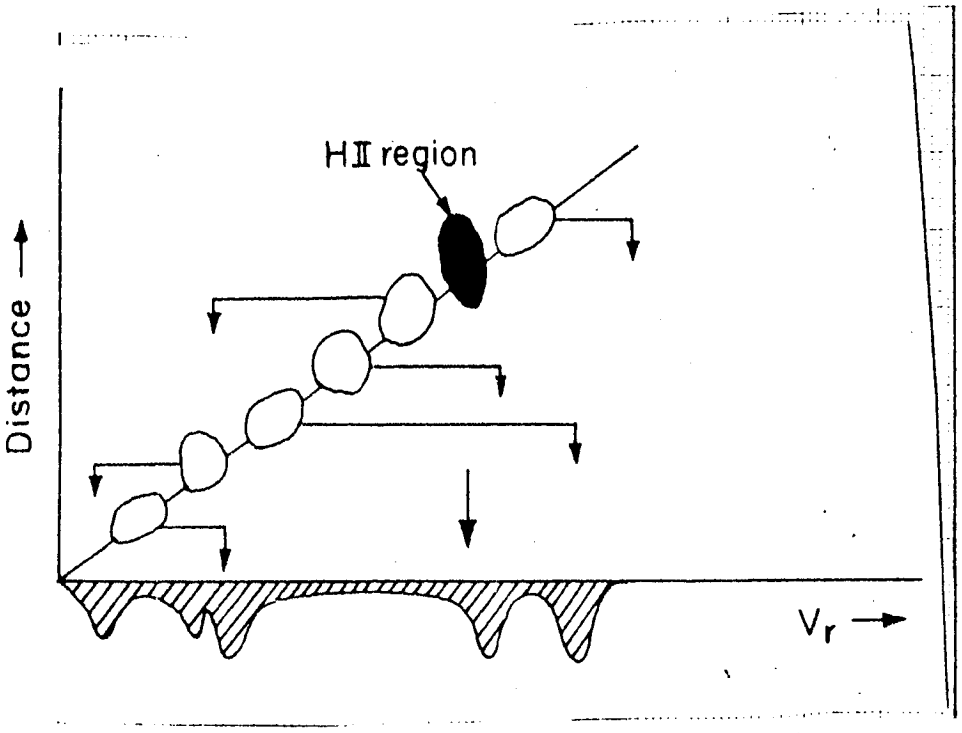

Figure 2. Schematic representation of radial velocity of HI clouds (unfilled blobs) lying along the line of sight to an HII region. The hatched curve represents the HI absorption spectrum in that direction. Note that the true order in distance of the clouds is replaced by their order in velocity in the absorption spectrum due to their random motions (arrows).

From many attempts to fit the histogram (Fig. 1) in terms of the random motions of HI clouds, it was concluded (paper I) that the histogram can be fitted in its entirety only on the assumption that there are two populations of HI clouds; the standard clouds easily seen in absorption and characterised by a gaussian velocity distribution with $\sigma \approx 5$ kms^{-1} ("slow"), and a smaller population with a much larger σ ("fast"). They also noted that while the dispersion of the slow clouds cannot be very different from the assumed value ($\sigma \approx 5$ kms^{-1}), there was considerable room (15-40 kms^{-1}) for varying the velocity dispersion and the number density of the fast population; when one was increased, the other had to be decreased to get a good fit to the histogram of Fig. 1.

In the simple analysis in paper I, average values for the velocity gradients and number densities were implicitly assumed. In this paper, we reanalyse the same data. In the next section, we investigate the effect of random motions and number densities of HI clouds on the expected velocity differences by taking into account the velocity gradient and distance of each individual HII region. In section III, we estimate the number densities and dispersion of random motions of the two populations of HI clouds from a least squares fit to the observed velocity differences ΔV. We also try a fit with a single exponential distribution of random velocities for the HI clouds, and show that even on the basis of this limited sample the two population hypothesis is to be preferred. Finally the implications of these results are discussed in section IV.

II. EFFECT OF VELOCITY GRADIENTS, DISTANCES AND RANDOM MOTIONS ON HII TERMINAL VELOCITIES

The influence of random motions on the velocity differences ΔV depends on the position of the HII region in the galactic disk as explained below. Consider for example an HII region in a direction close to that of the galactic centre for which the radial velocity gradient $|dv/dr|$ will be very small. In such a situation, and in the absence of random motions, most of the clouds along the line of sight to the HII region will have nearly the same velocity as the HII region itself. Given random motions, then in principle nearly half of these clouds can have velocities corresponding to a greater distance than the HII region. If the distance to the HII region were increased, then the number of clouds which could masquerade as being more distant than the HII region will increase. On the other hand, if the velocity gradient is very large, only a few clouds will have systematic velocities close to that of the HII region; but if the random velocities are large enough, then some of these clouds could have velocities corresponding to a greater distance than the HII region. In such a situation, increasing the distance to the HII region will have a negligible effect on the number of clouds which could appear as being more distant. In other words, a small $|dv/dr|$ coupled with a large distance is what is required for a clear manifestation of the random motions in this fashion.

We will now illustrate this effect with a few real cases taken from the sample of 38 HII regions. Following paper I, consider N HI clouds along the line of sight to an HII region. Let the velocity ΔV of the i^{th} HI cloud be governed by a gaussian distri-

bution with mean ΔV_i and standard deviation σ. ΔV_i is the systematic velocity difference between the HII region and the cloud. The probability distribution of ΔV_{max} corresponding to the terminal velocity of the spectrum is then given by

$$P(\Delta V_{max}) = \sum_{i=1}^{N} \left[p_i(\Delta V_{max} - \Delta V_i) \prod_{j \neq i}^{N} \int_{-\infty}^{\Delta V_{max}} p_j(\Delta V' - \Delta V_j)\, d\Delta V' \right] \quad (1)$$

$$\text{where } p_i(\Delta V - \Delta V_i) = \frac{1}{\sigma\sqrt{2\pi}} \exp - (\Delta V - \Delta V_i)^2 / 2\sigma^2$$

Eq. (1) is derived by assuming that any one of the clouds has a velocity ΔV_{max} and the remainder have smaller velocities. Suppose now there are N_s slow clouds characterised by a dispersion σ_s, and N_f fast clouds with a dispersion of σ_f. The over-all probability distribution of ΔV_{max} which we shall call ΔV is then given by

$$P(\Delta V) = \sum_{i=1}^{N_s} \left[p_{si} \prod_{j \neq i}^{N_s} \left\{ \int_{-\infty}^{\Delta V} p_{sj}\, d\Delta V' \right\} \prod_{k=1}^{N_f} \int_{-\infty}^{\Delta V} p_{fk}\, d\Delta V' \right]$$

$$+ \sum_{i=1}^{N_f} \left[p_{fi} \prod_{j \neq i}^{N_f} \left\{ \int_{-\infty}^{\Delta V} p_{fi}\, d\Delta V' \right\} \prod_{k=1}^{N_s} \int_{-\infty}^{\Delta V} p_{sk}\, d\Delta V' \right]$$

where $$p_{si} = p_{si}(\Delta V - \Delta V_i) = \frac{1}{\sigma_s\sqrt{2\pi}} \exp - (\Delta V - \Delta V_i)^2 / 2\sigma_s^2$$

and $$p_{fi} = p_{fi}(\Delta V - \Delta V_i) = \frac{1}{\sigma_f\sqrt{2\pi}} \exp - (\Delta V - \Delta V_i)^2 / 2\sigma_f^2$$

The N_s slow clouds and N_f fast clouds are assumed to be distributed uniformly but at random along the line of sight to the HII region. Then depending on its position, the systematic velocity difference ΔV_i for each cloud is given by the Schmidt model of galactic rotation. We derive in the Appendix a probability distribution eq (A1) for ΔV corresponding to eq (2) above, but taking full account of the distance and velocity gradient for each source. We show there that this is given by the convolution of a "window" function for each source with the probability distribution of peculiar velocities. Figs. 3 and 4 show the probability distribution functions $P(\Delta V)$ computed for 6 of the HII regions taken from Table 1, using the equation (A1).

The figures marked a1, a2, a3 show $P(\Delta V)$ computed using $N_s = 7.7\,d$ (where d is the distance to the source in kpc), $\sigma_s = 4.1$ kms^{-1} and $N_f = 0$ (only slow clouds); the figures marked b1, b2, b3 show $P(\Delta V)$ computed using the same values of N_s and σ_s but with $N_f = 0.6d$ and $\sigma_f = 15.2$ kms^{-1} (both slow and fast clouds). The choice of these numbers is explained in Section III. The figures marked c1, c2, c3 show the window functions $(1/|dv/dr|)$ as a function of velocity, and the arrows indicate the observed ΔV for the respective sources. G248.3-0.3 in Fig. 4 is an exam-

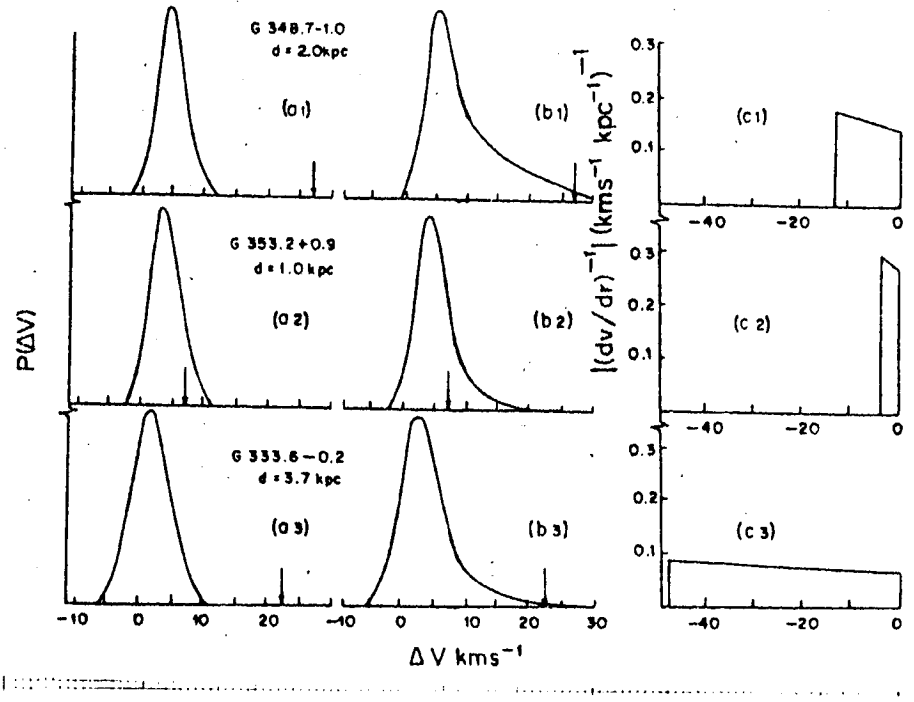

Figure 3. The overall probability distributions of ΔV for different HII regions. (a1), (a2), (a3) are the distributions computed assuming that only slow clouds are present along the line of sight; (b1), (b2), (b3) show the effect on the distribution of including fast clouds. (c1), (c2), (c3) are the window functions for the respective sources and represent the probability distribution of systematic velocity for each cloud along the line of sight, according to the Schmidt model (see Appendix). The arrows indicate the observed ΔV for the respective sources.

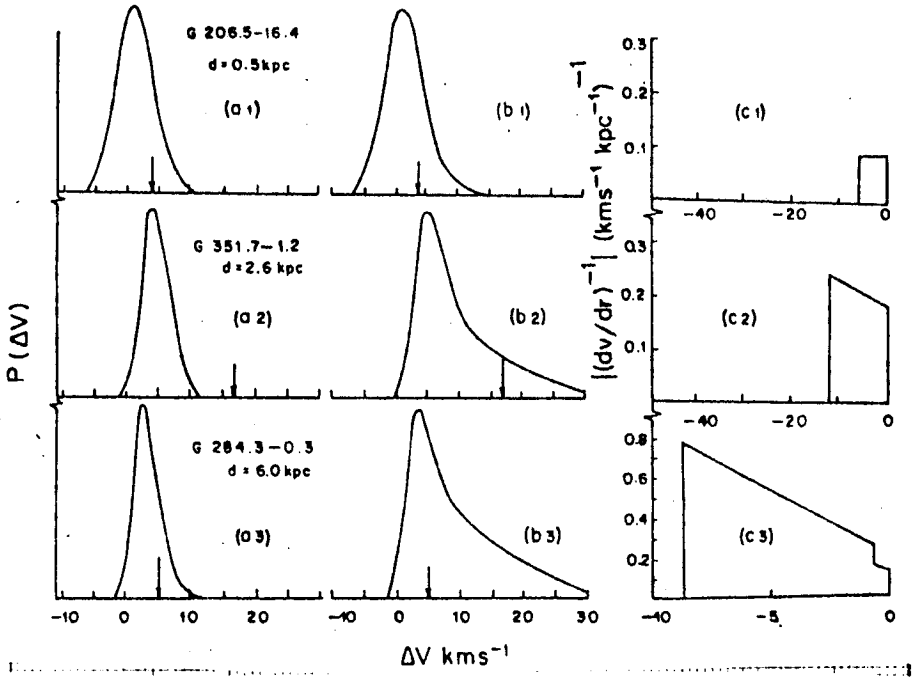

Figure 4. Same as Fig. 3. Note that for G284.3-0.3 which is outside the solar circle, the value of $(dv/dr)^{-1}$ is doubled for the region between the tangential point and the solar circle because of velocity folding (see Appendix).

ple of an HII region outside the solar circle for which the window function has a step at the solar circle velocity (see Appendix).

It is clearly seen in these figures that we cannot account for the high positive ΔV cases without introducing the second population of fast clouds with a high σ. It is also seen that dv/dr and the distances to the individual sources have in fact the expected effects on the probability distribution $P(\Delta V)$. The distributions and in particular their tails shift to more positive ΔV values as the area under the window function increases. For example, G348.7-1.0, G351.7-1.2 and G284.3-0.3, all of which have small values of $|dv/dr|$ and are at relatively large distance, have a long tail extending out to $\Delta V = 30$ kms^{-1}, whereas G353.2+0.9 although it has a small $|dv/dr|$, has a very low probability for high positive ΔV due to its small distance. On the other hand, G333.6-0.2 has a large $|dv/dr|$ but still has a tail in the distribution due to its large distance, and in fact the observed ΔV for this source is 21.7 kms^{-1}. For G206.5-16.4, the addition of fast clouds has a negligible effect on the $P(\Delta V)$ distribution due to its small distance and large $|dv/dr|$.

It should be pointed out here that $P(\Delta V)$ is only a probability distribution and therefore the presence of a long tail extending to large positive ΔV's does not require that for these sources the observed ΔV should necessarily be large. The presence of a long tail shows that there is a finite probability of observing a large positive ΔV, and for those sources for which the tail is absent the probability of observing a large positive ΔV is extremely small. We have examined these probability distributions for all the 38 HII regions in Table 1 and find that for all those cases in which high positive ΔV's are observed, the distributions indeed have long tails as for G348.7-1.0 and G333.6-0.2 in Fig. 3. For six of the sources for which the observed ΔV is negative, the distribution extends to negative ΔV's. It may be noted that for several sources the expected distribution is practically restricted to positive ΔV's only.

It is clear that these tests confirm the conclusions drawn in paper I where the sample was treated as homogeneous. It appears established that the random motions of HI clouds and their number densities manifest themselves in the observed differences between recombination line velocities and the velocities of the terminal HI absorption features. We can now ask how much more information we can get about these properties from the observed velocity differences in Table 1.

III. THE NUMBER DENSITY AND VELOCITY DISPERSION OF HI CLOUDS

It was shown in paper I and further confirmed from the tests described in Section II above that we need two populations of HI clouds with different random motions and number densities to account for the histogram of Fig. 1. If we assume that these two populations of HI clouds are randomly distributed throughout the Galaxy, we can then estimate the number densities (n_s and n_f) and velocity dispersions (σ_s and σ_f) from the observed ΔV's alone, to the accuracy permitted by the limited number in the sample.

Consider n_s slow clouds per kiloparsec with a dispersion σ_s, and n_f fast clouds per kiloparsec with a dispersion σ_f. Then the probability of observing a velocity dif-

ference ΔV is given by eqn. (A2) in which $N_s = dn_s$ and $N_f = dn_f$ where d is the distance to the source in kiloparsecs. If $\Delta V_1, \Delta V_2 \ldots \Delta V_{38}$ are the observed velocity differences for the 38 HII regions, then the individual probabilities of observing these differences are $P_1(\Delta V_1), P_2(\Delta V_2) \ldots P_{38}(\Delta V_{38})$. The joint probability of observing these velocity differences is

$$P = \prod_{i=1}^{38} P_i(\Delta V_i) \qquad (3)$$

We have maximised the quantity P by varying the four parameters n_s, σ_s, n_f and σ_f in an iterative procedure and obtained the best fit values. These values along with their errors and a measure of the goodness of fit are given in Table 2. (The estimation of errors and goodness of fit are discussed in Section II of the Appendix). These were the values of the four parameters that were used in the tests described in Section II. Fig. 5 shows the resulting predicted probability distribution (full line) for the histrogram computed using these parameters; the dashed line is the probability distribution computed using only one population of (slow) clouds ($n_f = 0$). It can be seen that as noted in paper I, the positive ΔV side of the histogram, including its long tail, requires the presence of the second population of fast clouds to give a good fit.

Table 2
Best fit values of HI cloud parameters

Velocity Distribution	Cloud population	Dispersion or scale length kms^{-1}	Number density kpc^{-1}	Ψ^2*
2 Gaussian	Slow	4.1±0.7	7.7±1.8	
	Fast	15.2±3.2	0.6±0.15	45.5
Exponential	Single	4.4±0.6	6.3±1.4	72.2

*Indicates goodness of fit (see Appendix).

It is interesting that the inability of a single gaussian to fit the peculiar motions of interstellar clouds was noted even in the earliest such study by Blaauw (1952) who analysed the measurements of Adams (1949) to determine the distribution of radial motions. He concluded that the high radial velocities observed for many clouds could be better accounted for by an exponential distribution of velocities for interstellar clouds. Both for the sake of completeness and for its appeal of simplicity, we have also considered here the possibility of a single population of clouds with an exponential distribution of velocities accounting for the observed high velocity differences shown in Table 1.

Consider again n clouds per kpc distributed randomly along the line of sight to

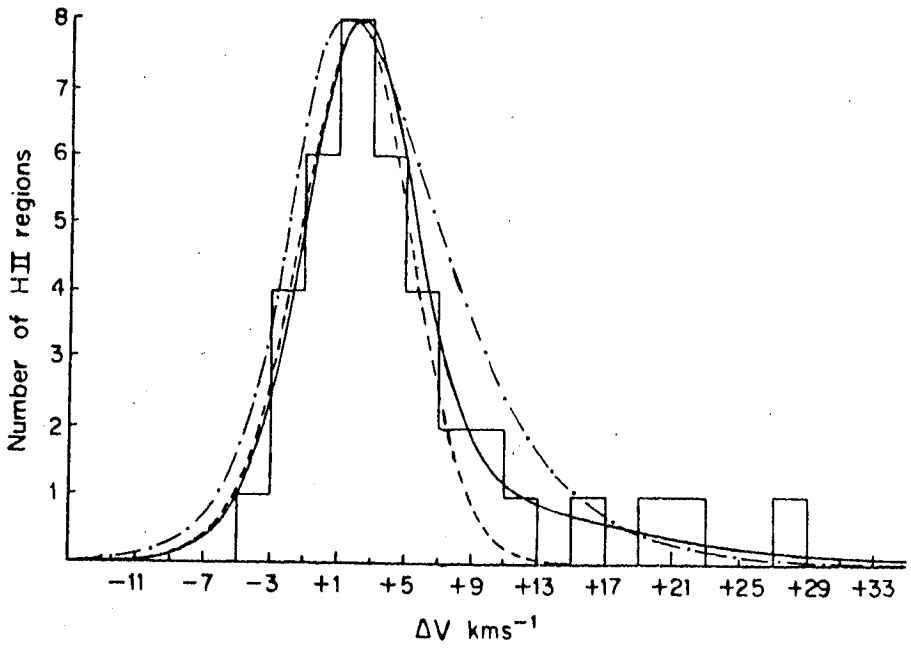

Figure 5. The composite probability distribution for ΔV obtained by adding the individual probability distributions for the 38 HII regions in the histogram, computed using the best fit values of the cloud parameters (Table 2). The full curve is the distribution computed using both slow and fast clouds. In the dashed curve the effect of fast clouds has been removed; the parameters for the slow clouds are as in Table 2. The dashed and dotted curve is the distribution computed using an exponential distribution of random velocities. Note that the curves are drawn with their peak values normalized to the peak of the histogram.

an HII region. Let the random velocity of each cloud be described by an exponential probability function of the form

$$P_{ran}(\Delta V - \Delta V_i) = A \exp(-|\Delta V - \Delta V_i|/\eta) \quad (4)$$

where η is the scale length of the distribution. As before, ΔV represents the difference between the velocity of the HII region and the cloud. The velocity distribution functions can be obtained in a similar fashion using equation (A1). Using these the probabilities P_1 (ΔV_1), P_2 (ΔV_2) . . . P_{38} (ΔV_{38}) can be obtained from eqn. (A2) by replacing N_s by nd (d is the distance to HII region in kpc), and setting $N_f = 0$.

We have again maximized the joint probability P (eqn. 3) in an iterative procedure by varying the parameters n and η. The best fit values of these parameters along with their errors and goodness of fit are given in Table 2. We have also shown in Fig. 5 the total probability distribution for the histogram computed on this basis (dots and dashes).

It can be seen both from Fig. 5 and from the goodness of fit values that the exponential distribution of radial velocities of a single population of HI clouds does not account for the observed velocity differences as well as the two-population hypothesis described earlier. It should be noted however, that the curves in Fig. 5 are a much poorer indication of the agreement between observation and prediction than the goodness of fit values. The latter represent a more stringent test involving the agreement in each individual case, as opposed to the general agreement with the total distribution of ΔV values in Fig. 5. Since it would be unwarranted at this stage to introduce more complicated distributions, we conclude from our analysis that the observed velocity differences in Table 1 can be best accounted for by two populations of HI clouds characterised by the number densities and velocity dispersions listed in Table 2.

IV. DISCUSSION

As noted in paper I, independent evidence indicating the presence of two populations of HI clouds has in fact been obtained from an investigation of the HI absorption spectrum towards the galactic centre, a direction free in principle of galactic rotation effects (Radhakrishnan and Srinivasan, 1980, hereafter R&S). These authors have also discussed even earlier evidence in the work of Routly and Spitzer (1952) and Siluk and Silk (1974), suggesting the existence of more than one population of interstellar clouds. While there is a qualitative agreement between the results obtained in Section III and the two-population picture of HI clouds proposed by R&S, there is considerable apparent disagreement in the number densities and dispersions, particularly those of the fast clouds. We shall discuss these discrepancies below.

Table 2 shows the characteristics of slow and fast clouds obtained from the analysis in Section III. While the slow clouds fall into the category of standard clouds very easily seen in 21 cm absorption studies and discussed by Radhakrishnan and

Goss (1972), the fast clouds may be tentatively identified with the "shocked clouds" with high random velocities discussed by R&S. Our value for the slow cloud number density of 7.7±1.8 kpc^{-1} is about 3 times that (2.5±.8kpc^{-1}) estimated from a statistical analysis of the Parkes 21 cm absorption survey (see Radhakrishnan and Goss, 1972 and references therein). It may seem intriguing at the outset that different number densities are obtained from two analyses of essentially the same data, since most of the HI absorption measurements of Table 1 were also taken from the Parkes survey (see paper I). However, the statistical analysis of Radhakrishnan and Goss (1972) suffered severely from blending of absorption features in velocity space as was noted by them.

If the number density of slow clouds is as high as indicated by the present analysis, then we may expect considerable blending of features in any HI absorption measurements irrespective of the velocity resolution used. Further, as discussed and emphasised by R&S, the estimates from optical observations have always been even higher, typically 10-20 kpc^{-1}. It is to be expected therefore that a gaussian analysis of the HI profiles would yield a smaller number density than the true value. In the present analysis of the differences in the velocity of the recombination line and that of the extreme HI *absorption* feature, we are working in a special region of velocity space where such blending is unlikely or very small. We therefore believe that our number density for the slow clouds is more accurate than earlier determinations.

While the velocity dispersion for the slow clouds obtained by us is in reasonable agreement with earlier determinations, it happens to be the smallest yet. The value of σ_s is 4.1+0.7 kms^{-1} as given in Table 2, whereas earlier estimates for it have been somewhat higher; for example, Crovisier (1978) obtained 5.7 ± 0.9 kms^{-1} (see that paper also for a discussion of previous determinations). Crovisier points out the difficulty of discriminating between a gaussian and an exponential distribution from his sample, and notes the presence of higher-velocity features the inclusion of which suggests the tail of an exponential. While choosing a gaussian distribution obtained by excluding these features, Crovisier in fact suggested that these higher-velocity clouds may belong to another population.

If there are really two populations, then it is only to be expected that the dispersion obtained by treating the data as belonging to a single population will tend to be higher through contamination of the sample. Radhakrishnan & Sarma (1980) quote a dispersion of 4.8 ± 0.2 kms^{-1} based on a gaussian analysis of the HI absorption profile towards Sgr A, and which refers to the slow clouds only. In spite of the errors in these various determinations, the trend is seen to be consistent with the two-population hypothesis. It must be mentioned here that in the present analysis we have consistently ignored the effect of any random motions associated with the HII regions themselves. If these are significant, the dispersions obtained by us will have to be reduced further; in any case, to within the errors, they may be considered upper limits.

We turn now to the fast clouds for which both our number densities and dispersions are substantially lower than the values suggested by R&S, $n_f \approx$ 15-20 kpc^{-1} and $\sigma_f \approx 35$ kms^{-1}. The discrepancies are so large that either one or both estimates

of each quantity are severely in error, or they do not refer to the same set of clouds. We discuss below a possible selection effect which could simultaneously explain the discrepancy in both the number density and the dispersion of the fast clouds.

There are a number of good reasons to believe that whatever mechanism accelerates the fast clouds – e.g. supernova shocks – will also heat and partially evaporate them (McKee and Ostriker 1977). Both the reduction in mass and increase in temperature will thus contribute to reducing the HI optical depth of the fast clouds. As discussed by R&S, there is also observational evidence supporting the correlation of high peculiar velocities with higher temperatures and lower optical depths in the measurements of Dickey et al (1978). As a direct result, any absorption survey will select only a fraction of the fast clouds whose optical depths (and corresponding mean speeds) are within the sensitivity limits of the survey.

The lowest optical depth of the features listed in Table 1 is 0.2, and the distribution of their optical depths indicates a sharp sensitivity cut-off around $\bar{\tau} \approx 0.3$. The median optical depth for the fast clouds is expected to be of the order of 0.1 or less (R&S). If the number of fast clouds as a function of their optical depth follows an exponential law as is true for the slow clouds (Clark 1965; Radhakrishnan and Goss 1972), then we should expect only a very small fraction ($\approx e^{-3} \approx 1/20$) of the fast clouds to appear in the data of Table 1. This is in reasonable agreement with the ratio of 0.6 kpc^{-1} found here, to 15-20 kpc^{-1} suggested by R&S.

The cut-off in peculiar velocity as a result of the same selection effect is not as easy to estimate because of the lack of a detailed theory relating cloud acceleration by shocks to their resultant HI optical depths. Even so, given that there exists a correlation of peculiar velocities with optical depth, it seems to us that the reduction in the observed dispersion ($15/35 \approx 40\%$) is not at all surprising for a sample of the optically thickest 5% of the total population of fast clouds. It should be noted that given a sensitivity cut-off, it would in general make it harder to distinguish between two gaussians and a single exponential for the total velocity distribution of the clouds. This has presumably contributed to the choice of an exponential distribution in some earlier analyses. In the present case however, goodness of fit tests, particularly on the tail of the histogram reject a single exponential distribution with more than 95% confidence.

In conclusion, the present analysis has demontrated that it can provide estimates of the number densities and random velocity dispersions of interstellar HI clouds. The novel method used here has the advantage of operating in a region of velocity space free of the blending effects which plague other types of analysis of similar observations in the galactic plane. The results support a two-population picture for galactic HI clouds. The values obtained here describing the population of slower and optically thicker clouds are believed to be better than other previous estimates. On the other hand, the number density and dispersion for the population of fast clouds are clearly underestimates because of a selection effect due to a sensitivity cut-off.

While it can be shown that the present and previous estimates for the numbers describing the fast clouds can be reconciled in terms of the selection effect, the overall uncertainties would not warrant an attempt to correct for it. If more sensi-

tive HI absorption measurements could be obtained near the terminal velocities of the spectra of even the present limited sample of sources, the parameters of the fast clouds could be well established. It would therefore be of value to carry out such measurements which we predict will reveal a number of low optical depth ($\tau < 0.1$) features located beyond the terminal velocities in the present data.

ACKNOWLEDGEMENTS

We thank Rajaram Nityananda and Ramesh Narayan for numerous discussions and helpful suggestions on the method of analysis.

APPENDIX

1. THE DISTRIBUTION OF CLOUD VELOCITIES

Consider a line of sight to an HII region along which the rate of change of radial velocity with distance (dv/dr) is a constant (the radial velocity increases or decreases linearly with distance). Then given a random distribution of N clouds along this line of sight, each of the clouds will have an equal probability of having any systematic velocity between 0 and the velocity of the HII region (V_{HII}). We ignore here large scale density fluctuations such as spiral arms, interarm regions, etc. Then, for each of the clouds the probability distribution of systematic velocity ia a rectangular (window) function extending from 0 to the velocity of the HII region.

The 38 HII regions in paper I were selected to all lie either much nearer than the tangential point or beyond the solar circle (otherwise ΔV values of both signs can occur even in the absence of random motions). If the HII region is outside the solar circle, the systematic velocity range is from the tangential point velocity (V_{TP}) to the velocity of the HII region, and each of the clouds will have twice the probability of having any systematic velocity between 0 and the tangential point velocity. In this case the probability distribution is a step function, the step being at the solar circle, viz. at a systematic velocity of 0.

Given a systematic velocity, the true velocity of the cloud will be given by a gaussian probability distribution function of dispersion σ centred on this systematic velocity. Clearly, the overall probability distribution for the velocity of any cloud is the convolution of the systematic velocity distribution and the random velocity distribution.

Mathematically, for any cloud the total probability distribution for the velocity difference between the HII region and it is given by

$$P_T(\Delta V) = P_{sys} * P_{ran} = \int_{-\infty}^{\infty} P_{sys}(\Delta V')\, P_{ran}(\Delta V - \Delta V')\, d\Delta V' \qquad (A1)$$

P_{ran} is the random velocity distribution given by

$$P_{ran}(\Delta V - \Delta V') = \frac{1}{\sigma\sqrt{2\pi}} \exp -(\Delta V - \Delta V')/2\sigma^2$$

P_{sys} is the systematic velocity distribution (the window function) obtained as described below.

In general, dv/dr varies as a function of distance (therefore as a function of velocity) and equal intervals in velocity space will not have equal probabilities. The probability of a cloud having a certain systematic velocity, and thus the number of clouds, will be inversely proportional to |dv/dr| at that velocity.

According to the Schmidt model of galactic rotation, 1/|dv/dr| varies smoothly as a function of distance (therefore as a function of velocity) except near the tangential point. If we ignore a small stretch near the tangential point, then the probability distribution function can be approximated by a trapezoidal window function. Some typical window functions are illustrated in Fig. 6. The one with a step is for an HII region outside the solar circle.

The probability distribution of ΔV for each of the clouds is then given by the

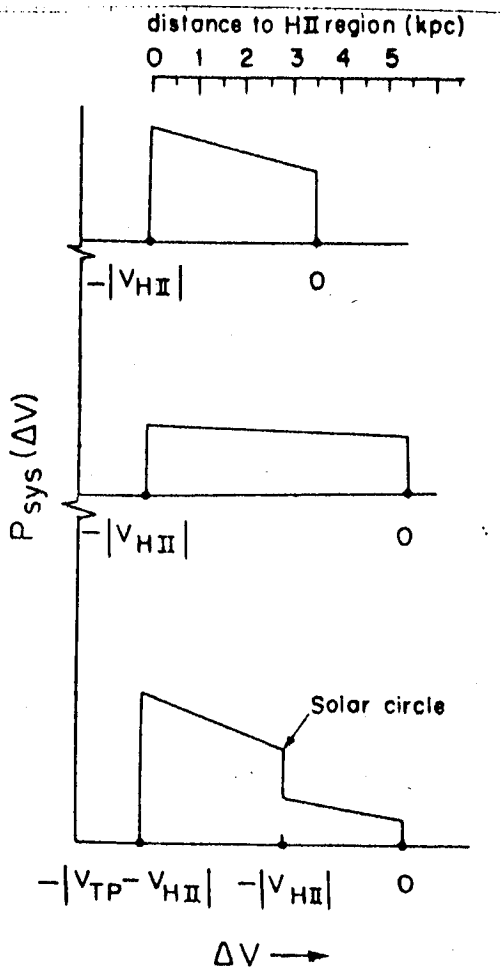

Figure 6. Typical probability distribution (the window function) of systematic velocity with respect to the HII region of any cloud lying along the line of sight to it. The one with a step is for an HII region outside the solar circle.

convolution of a trapezoidal window function such as shown in Fig. 6, with the gaussian probability distribution of peculiar velocities. If p_{Ts} is the total probability function of the fast clouds, then the equation (2) for the overall probability distribution of ΔV can be written as

$$P(\Delta V) = N_s P_{Ts} P_{T_s}^{N_s-1} P_{T_f}^{N_f} + N_f P_{Tf} P_{Tf}^{N_f-1} P_{T_s}^{N_s} \qquad (A2)$$

where $P_{Ts} = \int_{-\infty}^{\infty} P_{Ts}\, d\Delta V'$

$$P_{Tf} = \int_{-\infty}^{\infty} P_{Tf}\, d\Delta V'$$

Equation (A2) can now be used for computing the probability distribution of ΔV for individual HII regions. As noted earlier, if random motions of HI clouds are the origin of their apparently anomalous distances, we would expect a finite probability of finding large positive ΔV values for those HII regions which are distant and have a small $|dv/dr|$ along the line of sight. In other words, large positive values of ΔV can occur for those sources for which the window functions are of large widths or heights or both.

It should however be pointed out here that the exact probability distribution will depend on the number density and σ of the two populations. In the extreme case of very large number density and σ, there is always a high probability of large ΔV values irrespective of dv/dr and distance. But given reasonable number densities, and σ of the order indicated in paper I, we show in the text that the probability functions for ΔV in individual cases do indeed depend on the window functions.

2. GOODNESS OF FIT AND ESTIMATION OF ERRORS

To obtain the best fit values of the parameters n_s, σ_s, n_f and σ_f (or n and η for the exponential distribution) which correspond to the maximum value of the joint probability P (eqn. 3) we have minimized the quantity

$$-\log P = \sum_{i=1}^{38} -\log P_i(\Delta V_i) \qquad (A3)$$

The expectation value of $-\log P_i$ for the i^{th} HII region is given by

$$\langle -\log P_i \rangle = \int_{-\infty}^{\infty} (-\log P_i)\, P_i\, d\Delta V$$

and its variance is given by

$$\sigma_p^2 = \int_{-\infty}^{\infty} (-\log p_i - \langle -\log p_i \rangle)^2\, p_i\, d\Delta V$$

we define

$$\Psi^2 = \frac{N}{N-K} \sum_{i=1}^{38} (-\log p_i - \langle -\log p_i \rangle)^2 / \sigma_p^2 \qquad (A4)$$

where N-K is the number of degrees of freedom left after fitting K parameters to N data points (N=38).

The quantity Ψ^2 can be considered as a measure of goodness of fit and similar to the conventional χ^2. For a good fit the value of Ψ^2 must be close to N. The value of Ψ^2 computed using the best fit values for the two-gaussian and a single exponential distribution of velocities of HI clouds is given in table 2.

The parameters n_s, σ_s, n_f and σ_f (n and η for the exponential distribution) of the fit using the maximum likelihood method (of maximizing the joint probability P, eqn. 3) are not independent. The variation of -log P (eqn. A3) as a function of one of the parameters depends on how well the other parameters have been fitted. We have estimated the errors in each of the parameters assuming that the variation of -log P is parabolic, at least near its minimum, and taking into account the correlation between these variations with respect to different parameters. The errors quoted in table 2 correspond to one standard deviation.

REFERENCES

Adams, W.S., 1949, Astrophys. J., *109*, 354.
Blaauw, A., 1952, Bull astr. Inst. Netherl., *11*, 459.
Clark, B.G., 1965, Astrophys. J., *142*, 1398.
Crovisier, J., 1978, Astron. Astrophys., *70*, 43.
Dickey, J.M., Salpeter, E.E., Terzian, Y., 1978, Astrophys. J. Suppl. Ser., *36*, 77.
Mckee, C.F., Ostriker, J.P., 1977, Astrophys. J., *218*, 148.
Radhakrishnan, V., Goss, W.M., 1972, Astrophys. J. Suppl. Ser., *24*, 161.
Radhakrishnan, V., Sarma, N.V.G., 1980, Astron. Astrophys., *85*, 249.
Radhakrishnan, V., Srinivasan, G., 1980, J. Astrophys. Astr., *1*, 47.
Routly, P.M., Spitzer, L. Jr., 1952, Astrophys. J., *115*, 227.
Shaver, P.A., Radhakrishnan, V., Anantharamaiah, K.R., Retallack, D.S., Wamsteker, W., Danks, A.C., 1981, Astron. Astrophys. (to be published). *106*, 105
Siluk, R.S., Silk, J., 1974, Astrophys. J., *192*, 51.

DISCUSSION

Wynn-Williams: Could the presence of high velocity clouds have led to errors in the Schmidt rotation curve, which is based on HI velocities at the tangent points?

Answer : Yes, but whether the magnitude is significant is not yet clear. We are looking into it.